

## CFD-DEM INVESTIGATION OF PARTICLE SEPARATIONS USING A TRAPEZOIDAL JIGGING PROFILE

**Stephen VIDUKA<sup>1,2</sup>, Yuqing Q. FENG<sup>1\*</sup>, Karen HAPGOOD<sup>2</sup>, Phil SCHWARZ<sup>1</sup>**

<sup>1</sup> CSIRO Mathematics, Informatics and Statistics, Clayton, Victoria 3169, AUSTRALIA

<sup>2</sup> Monash Advanced Particle Engineering Laboratory,  
Department of Chemical Engineering, Monash University, Victoria 3800, AUSTRALIA

\*Corresponding author, E-mail address: Yuqing.Feng@csiro.au

### ABSTRACT

Jigging is one of the oldest methods of gravity separation and is still widely used in ore processing owing to its high separation precision, easy maintenance, cost-effectiveness and high throughput rate. This study investigates solid separation in a jigging device through a series of numerical simulations. The mathematical model adopted consists of computational fluid dynamics (CFD) coupled with discrete element method (DEM), which resolve the liquid and particle flow, respectively. Stratification is heavily influenced by fluid motion through the jig. Therefore, many jigging pulsation profiles have been developed and applied in ore processing. This study explores the trapezoidal pulsation profile adopting variations in amplitude and frequency. This aids in assessing how changes in profile affect jigging behaviour and also helps elucidate the governing concentration mechanics. The initial packing conditions consist of a binary-density particle system where the light particles and heavy particles have respective densities of 2540 and 4630 kg/m<sup>3</sup>. There are 1130 particles each 1 cm in diameter. Jigging profile performance is compared in terms of solid flow patterns, separation kinetics, energy, and mean particle position. Each variant demonstrates significant differences in segregation rate, solid phenomena, and energy consumption. These quantitative comparisons help find an optimum pulsation profile for the particle system. Further, boundaries of operation are investigated in terms of frequency and amplitude limits and the concentration mechanics in these regions are investigated.

### NOMENCLATURE

*A* cycle amplitude, L  
*f* contact, drag or gravitational force, N  
*g* gravitational acceleration, ms<sup>-2</sup>  
*I* rotational inertia momentum of particle, kgm<sup>2</sup>  
*k<sub>c</sub>* number of particles in a computational cell, dimensionless  
*k<sub>i</sub>* number of particles in contact with *i*, dimensionless  
*m* mass, kg  
*P* pressure, Nm<sup>-2</sup>  
*Q* volumetric flow rate, m<sup>3</sup>s<sup>-1</sup>  
*T* torque, Nm  
*T* cycle period, s  
*u* gas velocity, ms<sup>-1</sup>  
*v* solid velocity, ms<sup>-1</sup>

*V* volume, m<sup>3</sup>  
*ΔV* volume of computational cell, m<sup>3</sup>  
*ε* porosity, dimensionless  
*ρ* density, kg/m<sup>3</sup>  
*τ* continuum phase viscous stress tensor, kgm<sup>-1</sup>s<sup>-2</sup>  
*ω* rotational velocity of particle, s<sup>-1</sup>

### Subscripts

*c* contact  
*d* damping  
*f* fluid phase  
*i* particle *i*  
*j* particle *j*

### INTRODUCTION

Jigging is one of the oldest techniques used for gravity concentration, although currently the basic principles are not entirely understood. Jig units are widely used by the minerals industry to separate minerals from ore on the basis of particle size and/or density (Gupta, 2003). The method involves applying a pulsed liquid flow which dilates a particle bed and stratification ensues due to influences of hydrodynamic and gravity forces.

A vast majority of the research performed in jigging has been empirical (Kellerwessel, 1998). These studies are limited to the generation of macroscopic data. They do not elucidate on the intricate transient behaviour of the fluid and particles, along with separation kinetics which control the bulk behaviour of the process.

There are many numerical techniques that have been used to investigate jigging phenomena. Solnordal et al. (2009) applied a single phase computational fluid dynamic (CFD) technique but this was limited as it treated the slurry as a single phase. Various studies applied discrete element method (DEM) to simulate the motion of individual particles discretely coupled with simplified fluid models giving some insights into micro-mechanical processes at the particulate level (Beck and Holtham, 1993; Mishra and Mehrotra, 1998; Srinivasan, Mishra and Mehrotra, 1999; Mishra and Mehrotra, 2001; Mukherjee and Mishra, 2006; Mukherjee and Mishra, 2007). These modelling techniques assume a uniform fluid field and do not account for the effect of non-uniform fluid velocity on the particle drag forces. The Euler-Lagrange (DEM-CFD) model first proposed by Tsuji, Kawaguchi and Tanaka (1993), remains the most attractive technique because of

its superior computational convenience as compared to Direct Numerical Simulation-DEM, or Lattice Boltzmann-DEM models, and the capability to capture the particle physics as compared to DEM-simplified fluid models. The liquid phase flow is solved using the Navier-Stokes and continuity equations, while the motion of individual particles is obtained by solving Newton's second law of motion, with the liquid-particle coupling treated using Newton's third law of motion. This approach can generate detailed information about the trajectories of particles and the transient forces between two particles and between particles and fluid.

Only a few jiggling studies have adopted the DEM-CFD approach (Asakura et al., 2007; Xia and Peng, 2007; Dong et al., 2009). Both the studies by Asakura et al. (2007) and Xia and Peng (2007) are two-way coupled and consider drag on each particle individually, but do not consider porosity. Xia and Peng (2007) used a two dimensional (2D) column model and implemented forces including virtual mass force, Magnus force (Rubinow and Keller, 1961), and Saffman force (Saffman, 1965; Saffman, 1968). This study analysed the importance of different forces acting on a particle in jiggling and was performed for multi-sized and binary-sized particles in a sinusoidal pulsion. Additionally, the authors studied the hindered settling velocity as a function of particle densities and sizes, and the effect of sinusoidal pulsation, amplitude and frequency on the particle separation and fluid flows. Asakura et al. (2007) went a step further including the Basset force (Basset, 1961) and a three dimensional (3D) column model which studied the trajectory and response time of a single particle in a jig. Dong et al. (2009) applied a one-way coupled 3D model to a close-to realistic geometry Inline Pressure jig. The study considered that fluid flow is the dominant factor in the jig, and implemented a sawtooth-forward leaning jiggling profile investigating vibration frequency and amplitude, and the size and density of ragging particles on the flow separation. However, one-way coupling does not account for the influence of the local particles on the fluid.

Previous studies using the DEM-CFD model have used a sinusoidal pulsation profile with the exception of Dong et al. (2009), who used a forward leaning saw tooth cycle. No numerical investigations (including all various modelling techniques) have studied what effect the trapezoidal profile has on concentration mechanics. This study investigates the trapezoidal jiggling profile, with a mono-size binary-density system, using two-way coupling and a porous drag force model. The aim of this study is to elucidate how this profile induces segregation, and how variations of frequency and amplitude affect performance based on a range of criteria.

## MODEL DESCRIPTION

### Governing equations

The DEM-CFD model has been well documented in the literature. For brevity, only the outline of the model structure is described below. The solid phase is treated as a discrete phase and solved using DEM. The translational and rotational motions of a particle at any time,  $t$  (s), in the bed are determined by Newton's second law of motion. These can be written as:

$$m_i \frac{d\mathbf{v}_i}{dt} = \mathbf{f}_{f,i} + \sum_{j=1}^{k_i} (\mathbf{f}_{c,ij} + \mathbf{f}_{d,ij}) + \mathbf{f}_{g,i} \quad (1)$$

and

$$I_i \frac{d\boldsymbol{\omega}_i}{dt} = \sum_{j=1}^{k_i} \mathbf{T}_{ij} \quad (2)$$

The particle-particle and particle-wall contact force is based on the soft-sphere method. The particle fluid interaction force is calculated using the Di Felice drag force correlation (Di Felice, 1994), and Model B formulation is adopted (Feng and Yu, 2004). The lubrication squeeze mode, Magnus, Saffman, virtual mass and inertial forces were modelled but found sufficiently small to not be included in this study. The liquid phase is treated as a continuous phase moving through a porous medium created by the particles, and is modelled similarly to conventional two fluid models in which porosity (or liquid volume fraction) modifies the standard single phase Navier-Stokes equations. The governing equations are then the conservations of mass and momentum in terms of the local mean variables over a computational cell, given by:

$$\frac{\partial \varepsilon}{\partial t} + \nabla \cdot (\varepsilon \mathbf{u}) = 0 \quad (3)$$

and

$$\frac{\partial (\rho_f \varepsilon \mathbf{u})}{\partial t} + \nabla \cdot (\rho_f \varepsilon \mathbf{u} \mathbf{u}) = -\nabla P - \frac{\sum_{i=1}^{k_c} \mathbf{f}_{f,i}}{\Delta V} + \nabla(\varepsilon \boldsymbol{\tau}) + \rho_f \varepsilon \mathbf{g} \quad (4)$$

DEM is solved numerically with an in-house code using an explicit time integration method and established geometrical and flow boundary conditions. The continuous liquid phase is readily solved using a commercial CFD software package (ANSYS CFX 10.0). The two-way coupling between DEM and CFD is achieved as follows. At each time step DEM will give information of positions and velocities of individual particles for the evaluation of porosity and volumetric fluid drag force in a computational cell. CFD will then use this data to determine the fluid flow field, which in turn is used to determine the fluid drag forces acting on individual particles. Incorporating the resulting forces into DEM will produce information about the motion of individual particles for the next time step. The fluid drag force acting on an individual particle will react on the fluid phase from the particles, so that Newton's third law of motion is satisfied.

### Simulation conditions

The model consists of a rectangular domain filled with a binary-density spherical particle system and liquid. The particles were divided into 565 light particles (2540 kg/m<sup>3</sup>) and 565 heavy particles (4630 kg/m<sup>3</sup>), and the liquid was water (1000 kg/m<sup>3</sup>). Detailed model settings are shown in Table 1. The side walls were treated with no-slip

boundary conditions. The bottom was considered as a wall for the particle phase, so that so they cannot fall through, but as an inlet for liquid. The top exit was treated with a zero normal gradient opening condition. Periodic boundary conditions were applied to the front and rear surfaces of the flow domain effectively creating infinite thickness and economically reducing the number of particles required to produce three dimensional (3D) results. The liquid flow was considered in two dimensions (2D) using only one cell in the thickness direction and hence does not resolve detailed flow fields in this direction, while DEM modelling of the particles was in 3D, with a bed thickness equal to five particle diameters.

Uniform liquid flow was injected through the inlet and the flowrate varied with time according to the pulsation profile simulated. The inlet flow for the trapezoidal pulsation profile was established using a heavy side step function. The pulsation profiles are compared by holding the shape of the profile constant and using 3 variations of period ( $T$ ) and volumetric water input/exhaust ( $A$ ). These are 1, 2, and 3 second periods, and, 1.5, 2.25 and 3 litre water amplitudes. An example of the trapezoidal profile is displayed graphically in Figure 1. Each profile includes a pulsion period with an upward liquid motion (positive value in velocity) and a suction period with a downward liquid motion (negative value in velocity). The simulation begins with the random generation of particles followed by a period of gravitational settling to form an initial mixed packed bed. During the settling process the buoyancy force to particles is switched off to help prevent segregation during settling before jiggling commences. After settling, liquid is injected through the bottom following the appropriate pulsation profile, and jiggling begins. The jiggling process was concluded with 1 second of settling after the last jiggling cycle.

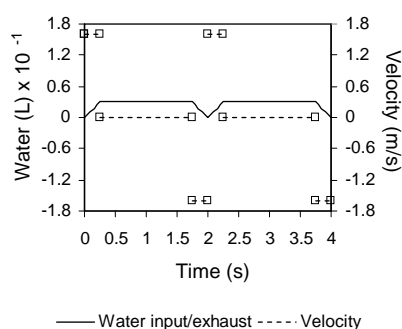


**Figure 1:** An example of the trapezoidal pulsation profile applied at inlet boundary condition.  $T=2$  s,  $A=3$  L

Particle phase		
Density ( $\text{kgm}^{-3}$ )	Light	2,540
	Heavy	4,630
Young's Modulus ( $\text{Nm}^{-2}$ )	1.0 $\times 10^8$	
Poisson ratio ( $\text{Nm}^{-2}$ )	0.3	
Sliding friction coefficient (-)	0.3	
Damping coefficient (-)	0.2	
Particle diameter (m)	Light	0.01
	Heavy	0.01
Number of particles (-)	Light	565
	Heavy	565
Time step (s)	1 $\times 10^{-5}$	

Liquid phase		
Viscosity ( $\text{kgm}^{-1}\text{s}^{-1}$ )		1 $\times 10^{-3}$
Density ( $\text{kgm}^{-3}$ )		1000
CFD Cell (m)	Width	0.025
	Height	0.025
Bed Geometry (m)	Width	0.15
	Height	0.9
	Thickness	0.05
Bed distributor		Uniform
Time step (s)		1 $\times 10^{-3}$

**Table 1:** Jiggling model specifications.

## RESULTS

### Solid Flow Patterns

Solid flow patterns are plotted to obtain a visual understanding of the stratification process. Figure 2 shows the particle positions for the trapezoidal profile variant of  $T=2$  s and  $A=3$  L over six jiggling cycles. This variant elucidates on more general profile phenomena which exist in all the profile variants. The maximum and minimum particle displacements can be visualized. The light particles are coloured black and heavy particles grey. Three snapshots are taken at each cycle: before pulsion, during the cycle at maximum particle height, and at the end of suction, respectively.

The initial cycle of the trapezoidal profile in all variants begins well mixed and expands vertically in almost a uniform manner (see Figure 2). The high injection liquid velocity tends to cause the bed to completely lift off the bottom of the jig to great heights. As segregation progresses the particles at the top of the bed cluster together and lift increasingly as one whole and to greater heights. Alternatively, reverse segregation is shown to be possible, during the 6<sup>th</sup> cycle particles mix and the bed consequently lifts to a lower height (see Figure 2). Further, immediately as the bed begins to lift particle loosening is present at the bottom which propagates upwards and aids in expanding the bed. This loosening wave arises from the interfacial instability at the bottom of the bed and fluid interface which causes particles to 'rain' down (Gibilaro, 2001).

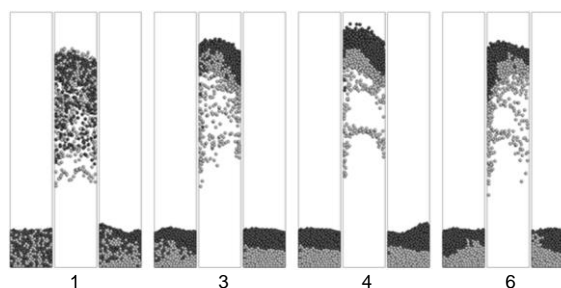


**Figure 2:** Solid flow patterns shown by particle position for variant  $T=2$  s,  $A=3$  L, at the: 1<sup>st</sup>, 3<sup>rd</sup>, 4<sup>th</sup>, and 6<sup>th</sup> cycle. Heavy and light particle are coloured grey and black respectively.

The mean particle position can be used to quantify particle behaviours by illustrating the average height of

both particle types separately. Figure 3 shows the mean particle position for the trapezoidal profile variant of  $T=2$  s and  $A=3$  L over 12 seconds of jigging. Starting from a well mixed state where each type of particle has a similar mean position, the light and heavy particles travel upwards at a similar velocity and reach almost identical heights. This indicates the bed is travelling relatively as one mass upwards irrespective of particle density, and that little or no segregation eventuates. During the settling and suction period after pulsion the heavier particles settle much quicker than the light particles. This is heavily influenced by the large period of zero inlet velocity between pulsion and suction. Here particles settle relatively slowly in the absence of suction and achieve terminal velocity. As the heavy particles have a higher terminal velocity, and this period is present for a great amount of time, they settle faster and reach the bottom of the jig much earlier. In addition, as segregation progresses the heavy particles are increasingly situated closer to the bottom of the column and thus have less distance to travel and increasingly settle quicker.

Following jigging more and more light particles aggregate on top of heavier particles. As this occurs lighter particles receive less constraint from the heavier particles and are able to travel higher in proceeding jigging cycles until a dynamically stable state is reached or segregation is reversed and mixing occurs. The peak mean position is shown to drop after 8 seconds during the 5<sup>th</sup> cycle (see Figure 3). After 8 seconds minor bed circulation ensues during settling which corresponds to mixing. The growing differences in mean particle positions display gradual segregation up to 8 seconds into jigging.

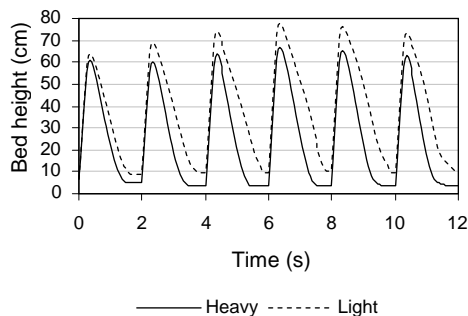


**Figure 3:** Mean particle position for variant  $T=2$  s,  $A=3$  L.

The maximum particle displacements of all variants in the first cycle can be visualized in Figure 4, together with the particles in a rested state once segregation is achieved. The results show vast differences in maximum heights the particles reach in pulsion and also differences in bed expansion.

It can be seen profiles with volumetric water inputs of  $A=1.5$  L, do not lift the bed to great heights due to a low inlet velocity and therefore drag force upwards. Consequently, there is little opportunity for bed expansion and little differential settling time which facilitates particle rearrangement. These variants generally require a lot of time to segregate the particle bed. Alternatively, it can be seen as the volumetric input increases the bed maximum particle height, and thus differential settling and expansion increases. This is advantageous to segregation, and these profiles segregate much faster.

Increasing frequency has a similar effect of increasing volumetric input, where the bed is increasingly lifted

higher due to an increase in inlet velocity and separation is faster.

However, as particles settle slowly due to a zero inlet velocity in the midst of the cycle, when a high frequency and high volumetric input is adopted the particles do not form a fixed bed before pulsion in the following cycle (see variant  $A=2.25$  L and  $A=3$  L on the bottom of Figure 4 (a), where particles are shown to be far from settled at the end of suction). Consequently, the particles undergo pulsion in an already suspended and relatively high voidage state which leads to bed circulation and mixing. These variants cannot successfully induce segregation.

Therefore, a profile must sufficiently lift the bed to a height where expansion and loosening can proceed, and differential settling time will be high, but also must allow the bed to settle or be close to settled.

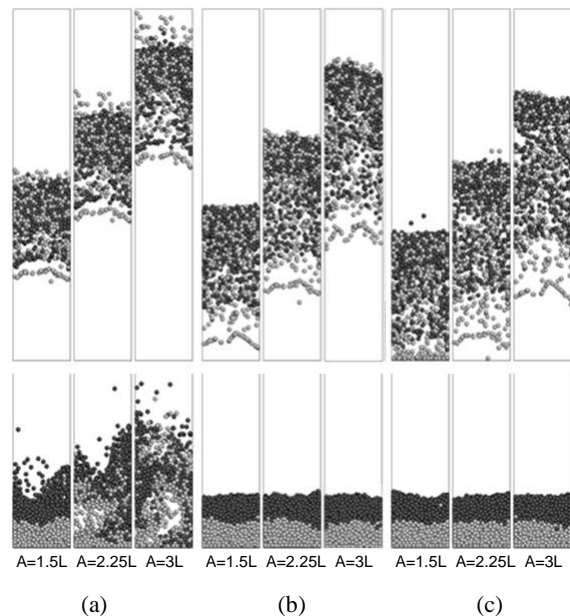


**Figure 4:** Solid flow patterns at maximum particle height in the first cycle for all variants of the trapezoidal profile (top) and snapshots at a rested state on completion of separation (bottom). Heavy and light particle are coloured grey and black respectively. (a)  $T=1$  s, (b)  $T=2$  s, (c)  $T=3$  s

#### Particle Separation Speed

The coordination number represents the average sum of contacts of a particle type, with either similar or different particle types. The heavy-light coordination number is a good indication of particle segregation. The value gradually reduces from when the bed is in a mixed state through to complete segregation, the lower the value the higher the segregation i.e. the less light particles are in contact with heavy particles.

The coordination number fluctuates as the bed expands under pulsion and compacts under suction. Only values when the bed is at rest are considered which coincides with the state of the final product.

Of the nine profiles, seven completely segregated the particle bed. Complete segregation is indicated by a plateau in the coordination number after approximately a value of 0.5, slight differences under this value are insignificant (see Figure 5). Steady separation is critical for a reliable jigging process. The separation process can be unsteady and is able to reverse and mix in subsequent

cycles, in this situation the coordination number of a rested bed will fluctuate (Viduka et al., 2011). In this study the trapezoidal profile is found to provide steady segregation for only four variants.

A consistently low coordination number indicates stable separation and a segregated bed. However, it does not characterize in which way particles have settled. Desirable settling occurs when particles are stratified vertically with one particle type directly on top of another, this ensures separate delivery to launders. In addition to segregation the settling also needs to be stable. If settling is inconsistent it is undesirable and unreliable in jig processing even if the bed is perfectly segregated. The solid flow patterns, as in Figure 2, help visualize the settling behaviour. Similar to the coordination number the solid flow pattern is tracked through all the jiggling cycles, if a tendency of undesirable settling is present the variant is deemed impractical for particle processing of this system. Only three variants of the trapezoidal profile were found to behave steadily in both coordination number and settling configuration.

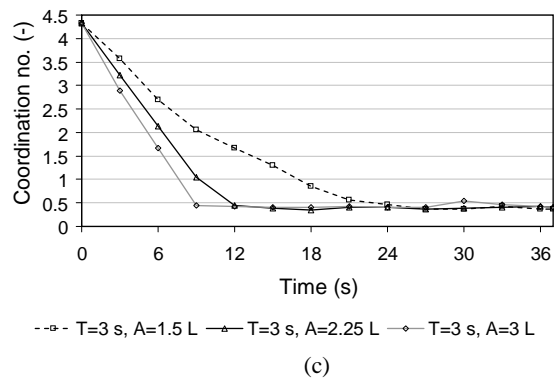
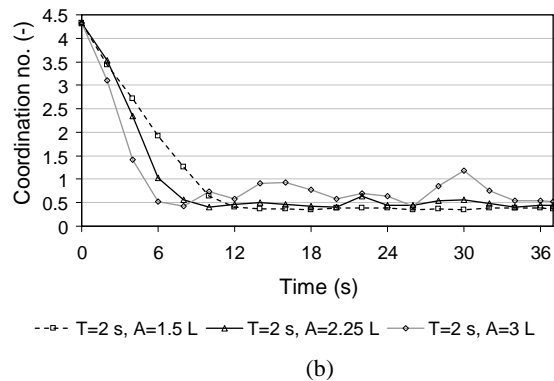
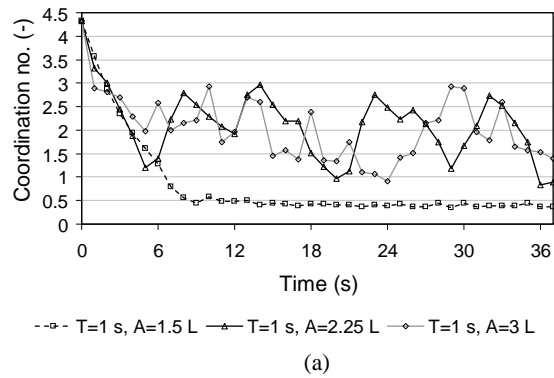


**Figure 5.** Packed bed coordination number values for all profile variants. (a)  $T=1$  s, (b)  $T=2$  s, (c)  $T=3$  s

The effects of volumetric water input and cycle period on the separation time is shown in Figure 6. Here a broader profile parametric study was conducted where the profile settings ensured stable separation in both coordination number and settling configuration. This helps illustrate the complete particle separation time phenomenon in terms of amplitude and frequency selection. A strong relationship between volumetric input and separation time is seen in all variants of frequency (Figure 6 (a)). As amplitude increases the separation time almost linearly reduces. Increasing frequency has a similar effect of increasing amplitude, separation time almost or does linearly reduce (see Figure 6 (b)).

Further, the ‘filled-in’ data points in Figure 6, which occur at the lowest separation time indicate the operational limit. Whereby an increase in either  $A$  or reduction in  $T$  will result in unstable segregation. Conversely, reducing  $A$  or increasing  $T$  will slow segregation up until the inlet velocity is insufficient to dilate the particle bed.

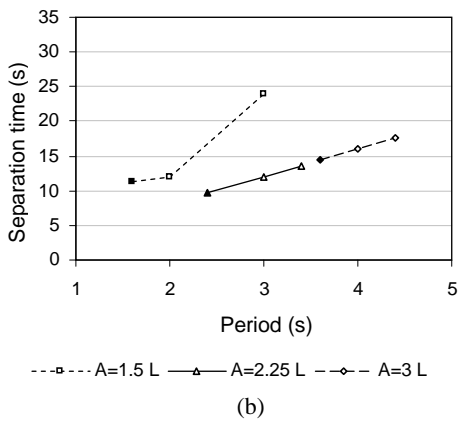
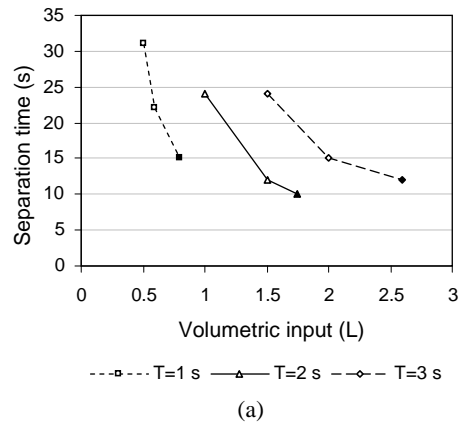


**Figure 6.** The effect of separation time against pulsation profile input parameters. (a) Volumetric input, (b) Cycle Period

The number of jiggling cycles used to achieve segregation can be important in terms of operating wear and fatigue. High cycle numbers may cause certain mechanical damages earlier. The two profile variants,  $T=1$  s and  $A=0.8$  L, and,  $T=3$  s and  $A=2$  L, both segregate in 15 seconds. However, the high frequency profile of  $T=1$  s requires 10 additional cycles to perform, that is 200% more cycles.

### Jigging Profile Optimisation

The mean particle positions for all of the successfully segregating profiles remain at a constant value for a significant amount of time. These moments correspond to a fixed bed which is a waste of time and energy as the particles are ready for subsequent pulsion. Therefore, an opportunity to improve jigging performance by modifying the profile settings exists. Figure 7 (a) displays the mean particle position for a high frequency variant of  $T=1$  s where the mean particle position is constant for the shortest time of all variants. Figure 7 (b) displays values for a low frequency profile of  $T=3$  s where the bed remains in a static state for a very long time. Moreover, it is shown in both variants that the bed comes to rest before suction begins, rendering this portion of the cycle redundant.

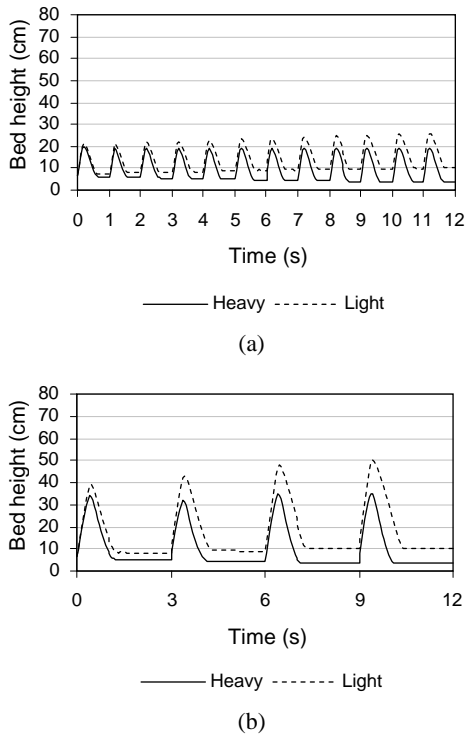


**Figure 7:** Mean particle position showing where profile improvements can be made.  
(a)  $T=1$  s,  $A=0.8$  L, (b)  $T=3$  s,  $A=2.25$  L

Using mean particle position data to identify at what point in the cycle the bed comes to rest, this point was made the beginning of the following cycle. To illustrate how the profile setting can be improved the settings were changed for the profile of  $T=3$  s and  $A=2.25$  L shown in Figure 7 (b). The original variant period,  $T$ , of 3 seconds was changed to 1.75 seconds and as a consequence suction is completely removed and water input is not exhausted at the conclusion of the cycle. This has no influence on results, but can be a consideration for jigging design, the inlet and mid-cycle water velocity remains the same. Figure 8 (a) shows the modified profile setting. The resulting mean particle position is shown in Figure 8 (b) where there is a reduction in time the bed is at rest when compared to Figure 7 (b). After modification the profile separated after 7 seconds, which is 5 seconds (42%) faster. It would be expected that the fastest profile is the most efficient segregator in terms of time. Applying the same treatment to the fastest profile of  $T=2.4$  s and  $A=2.25$  L,

the profile separated 2.8 (29%) seconds faster. All other profiles have the ability to increase performance in terms of segregation speed, while the cycle numbers remain the same.

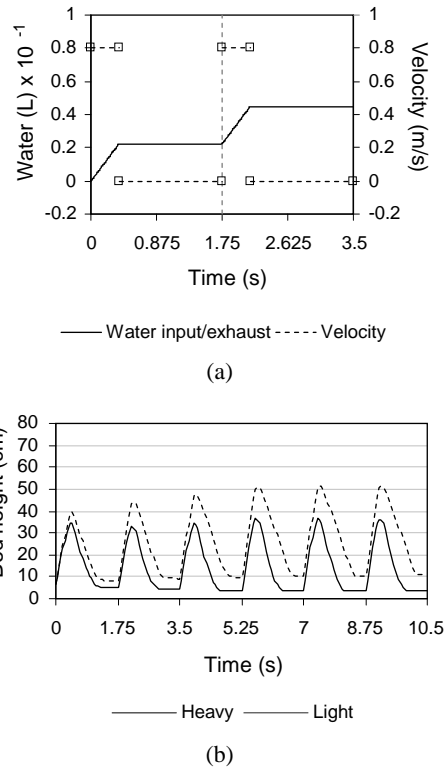


**Figure 8:** Alternative profile.  
(a) Improved profile setting, (b) Mean particle position of improved profile

### Power

There are various parameters to judge the performance of a jigging device. In addition to the separation speed, number of cycles to achieve segregation, and the final degree of separation as already discussed, the energy input is an important concern in industrial processes.

The following formula is used to calculate the input power, where power is a product of total pressure drop  $\Delta P_t$  and volumetric flow rate  $Q$ :

$$Power = \Delta P_t Q \quad (9)$$

and

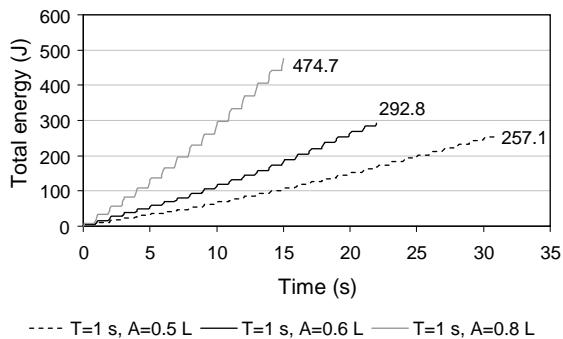
$$\Delta P_t = \Delta P_{fa} + \Delta P_{pa} + \Delta P_{fw} + \Delta P_{sw} + \Delta P_{shs} + \Delta P_{shf} \quad (10)$$

where the total pressure drop  $\Delta P_t$  is a summation of various pressure drops due to,  $\Delta P_{fa}$ , fluid acceleration,  $\Delta P_{pa}$ , particle acceleration,  $\Delta P_{fw}$ , fluid-to-wall friction,  $\Delta P_{sw}$ , solid-to-wall friction,  $\Delta P_{shs}$ , static head of solids, and,  $\Delta P_{shf}$ , static head of fluid. The contributions of wall effects are not resolved in high resolution using the current model due to the computational effort and complexity. Although these effects do contribute they are relatively small. The following power values are

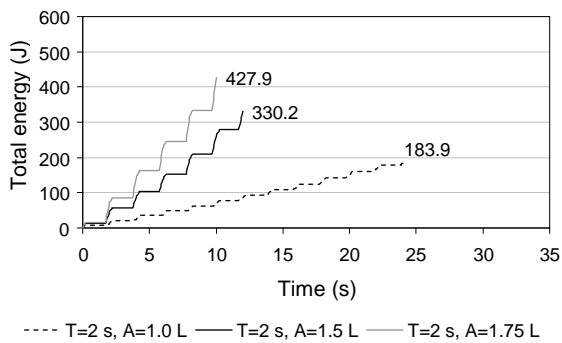
calculated using ANSYS CFX 10.0 commercial software. The values calculated are not absolute power values yielding only qualitative results. The model does not consider the fluid pushing through a distributor plate at the inlet which would cause substantial drag on the fluid. By integrating power over the jiggling time the total energy can be calculated shown in Figure 9.

The results show energy per cycle is proportional to water volumetric input. Further, it is shown that for a constant cycle period energy used to complete segregation is directly proportional to volumetric input. When considering all the cycle periods and volumetric inputs together, the energy required is shown overall not to be dependent on the time taken to achieve segregation. A profile can use little or a large amount of energy and segregate either quickly or slowly. Each profile has individual characteristics and reasons which describe the energy required to achieve segregation. There is no correlation between the profiles which can be used as a quick aid for power evaluation. For example, neither: litres input, segregation speed, pulsion or suction velocities or duration, alone correlate to the total energy used. It is a combination of all these variables which decide the energy outcome.

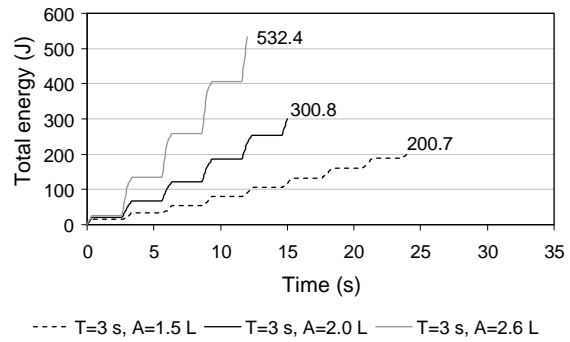
Further, as the particle bed in all profile variants falls to rest before suction initiates, the bed undergoes suction in a packed state. Due to the low voidage in the packed bed and high suction velocity in all profiles, a high pressure drop is present which results in very large energy consumption. Optimising the profile as mentioned previously by reducing the time the bed is at rest will eliminate this redundant power consumption.



(a)



(b)



(c)

**Figure 9:** Total energy for all variants.

(a)  $T=1$  s, (b)  $T=2$  s, (c)  $T=3$  s

## CONCLUSION

Gravity concentration in a jiggling device using the trapezoidal profile has been studied with a DEM-CFD model. The study initially selected three variations in amplitude and applied those over three frequencies. A number of the variants induced particle separation, but displayed differences in separation rate and power usage. Alternatively, two variants exhibited bed circulation and mixing due to the particles not having enough time to settle before subsequent pulsion. Segregation was found to be primarily active after pulsion while the particles differentially settled.

Of the nine variants only three displayed stable separation which was illustrated by a plateau in the coordination number, and through stable vertical separation shown in the solid flow patterns.

A broader jiggling profile parametric study in terms of amplitude and frequency values was performed for the purpose of a deeper investigation and to establish operational limits of these parameters. It was found increasing amplitude induces faster separation regardless of the frequency adopted. However, an upper limit to the amplitude adopted exists where particle bed settling becomes unstable. Here the particles do not stratify vertically with one particle type directly on top of another, and thus does not ensure separate delivery to launders. Alternatively, reducing the amplitude will increase separation time until the inlet velocity provides insufficient drag to dilate the bed. Increasing frequency displayed the same effects as increasing amplitude.

The number of cycles used to complete separation is found to be vastly different and could be a consideration in operation. Two profiles which complete segregation in 15 seconds were found to do so with a 200% difference in jiggling cycle numbers.

The mean particle position for all profiles indicate that the particle bed falls so rest in the midst of a cycle (after pulsion but well before suction). This static moment is a waste of processing time and indicates that suction is not necessary in this system. By eliminating this period the separation time is found to reduce significantly. The variant investigated separated 42% faster.

Finally, the total energy and time required to complete separation are not dependent on one another. It is a combination of many factors which contribute to the final energy outcome e.g. water velocity, pulsion duration, and separation time. Additionally, as particles completely fall to rest before suction commences, the suction imparts a

high negative liquid velocity on a packed bed resulting in a large pressure drop and high power consumption. Eliminating the suction portion of the cycle not only reduces separation time but largely reduces power usage.

## REFERENCES

ASAKURA, K., MIZUNO, M., NAGAO, M. and HARADA, S., (2007), "Numerical Simulation of Particle Motion in a Jig Separator", *5th Joint ASME/JSME Fluids Engineering Conference*, San Diego, California USA.

BASSET, A. B., (1961), "*Treatise on hydrodynamics*". Cambridge, Deighton, Bell and Co., 2.

BECK, A. J. G. and HOLTHAM, P. N., (1993), "Computer simulation of particle stratification in a two-dimensional batch jig", *Minerals Engineering*, **6**(5), 523-532.

DI FELICE, R., (1994), "The voidage function for fluid-particle interaction systems", *International Journal of Multiphase Flow*, **20**(1), 153-159.

DONG, K. J., KUANG, S. B., VINCE, A., HUGHES, T. and YU, A. B., (2009), "Numerical simulation of the in-line pressure jig unit in coal preparation", *Minerals Engineering*, **23**(4), 301-312.

FENG, Y. Q. and YU, A. B., (2004), "Assessment of model formulations in the discrete particle simulation of gas-solid flow", *Industrial and Engineering Chemistry Research*, **43**, 8378-8390.

GIBILARO, L. G., (2001), "*Fluidization - Dynamics*", Butterworth - Heinemann, 44 -46.

GUPTA, C. K., (2003), "*Chemical Metallurgy: Principles and Practice, Chapter 2: Mineral Processing*", Weinheim: Wiley-VCH,

KELLERWESSEL, H., (1998), "Concentration by jigging—current investigations, concepts and models", *Aufbereitungs-Technik* **39**(1), 9-15.

MISHRA, B. K. and MEHROTRA, S. P., (1998), "Modelling of particle stratification in jigs by the discrete element method", *Minerals Engineering*, **11**(6), 511-522.

MISHRA, B. K. and MEHROTRA, S. P., (2001), "A jig model based on the discrete element method and its experimental validation", *International Journal of Mineral Processing*, **63**(4), 177-189.

MUKHERJEE, A. K. and MISHRA, B. K., (2006), "An integral assessment of the role of critical process parameters on jigging", *International Journal of Mineral Processing*, **81**(3), 187-200.

MUKHERJEE, A. K. and MISHRA, B. K., (2007), "Experimental and simulation studies on the role of fluid velocity during particle separation in a liquid-solid fluidized bed", *International Journal of Mineral Processing*, **82**(4), 211-221.

RUBINOW, S. I. and KELLER, J. B., (1961), "The transverse force on a spinning sphere moving in a viscous fluid", *Journal of Fluid Mechanics (1961)*, **11**, 447-459.

SAFFMAN, P. G., (1965), "Lift on a small sphere in a slow shear flow", *Journal of Fluid Mechanics*, **22**, 385-400.

SAFFMAN, P. G., (1968), "Corrigendum to "The lift on a small sphere in a slow shear flow"", *Journal of Fluid Mechanics*, **31**, 624.

SOLNORDAL, C. B., HUGHES, T., GRAY, A. H. and SCHWARZ, P. M., (2009), "CFD Modelling of a Novel Gravity Separation Device", *Seventh International Conference on CFD in the Minerals and Process Industries*, CSIRO, Melbourne, Australia.

SRINIVASAN, R., MISHRA, B. K. and MEHROTRA, S. P., (1999), "Simulation of particle stratification in jigs", *Coal Prep.*, **20**, 50-70.

TSUJI, Y., KAWAGUCHI, T. and TANAKA, T., (1993), "Discrete particle simulation of two-dimensional fluidized bed", *Powder Technology*, **77**(1), 79-87.

VIDUKA, S., FENG, Y., HAPGOOD, K. and SCHWARZ, M. P., (2011), "Discrete particle simulation of particle separation in a Jigging device", *The 4th Conference on Industrial Fluidization*, Gauteng, South Africa.

XIA, Y. K. and PENG, F. F., (2007), "Numerical simulation of behavior of fine coal in oscillating flows", *Minerals Engineering*, **20**(2), 113-123.